Int. J. Heat Mass Transfer. Vol. 30, No. 8, pp. 1595–1606, 1987
Printed in Great Britain

0017–9310/87 $3.00 + 0.00

Heat and mass transfer in a non-isothermal fixed bed solid adsorbent reactor: a uniform pressure–non-uniform temperature case

J. J. GUILLEMINOT and F. MEUNIER
Laboratoire de Thermodynamique des Fluides, Campus Universitaire, Bat. 502 Ter, 91405 Orsay Cedex, France

J. PAKLEZA
L.I.M.S.I. (CNRS), Campus Universitaire, Bat. 508, 91405 Orsay Cedex, France

(*Received* 8 *December* 1985 *and in final form* 6 *October* 1986)

Abstract—A uniform pressure model is presented to describe the heat and mass transfer in a fixed bed of solid adsorbent in a finned reactor. This model neglects the resistance to mass diffusion but takes into account the resistances to heat diffusion through two coefficients: the heat conductivity of the adsorbent bed and the heat transfer coefficient between the adsorbent bed and the fins. An experiment has been conducted to validate this model and the two heat transfer coefficients are obtained by an identification technique. When the temperature of the closed reactor is modified on one side of the reactor, large temperature inhomogeneities inside the reactor are observed and mass transfer occurs through a heat pipe effect: the model explains that effect which is observed experimentally. That uniform pressure model is more adapted to describe the history of solid adsorbent reactors used in thermal processes than uniform temperature models proposed by other authors.

1. INTRODUCTION

HEAT AND mass transfer on fixed bed solid adsorbents have, up to now, mainly been studied in the case of uniform temperature when the bed diffusion controls the kinetics [1].

In this paper, we address the problem of the kinetics of sorption in a non-uniform temperature field.

Let us first present the experimental cell which has been used and which corresponds to a case when the conduction through the bed controls the kinetics of sorption.

Figure 1 shows the copper reactor that has been studied in our laboratory and is analogous to those used in the solar-powered ice-making unit [2]. The characteristics of this experimental cell are the following (Fig. 1):

surface: 0.25 m^2
length: 0.50 m
thickness: 0.10 m
fin 0.09 m high and 0.001 m thick
space between fins: 0.05 m.

A mass of 10 kg of A.C. 35 activated carbon in the form of pellets 1 mm diameter is distributed between the fins. A free space is created at the bottom of the reactor to allow better distribution of vapour through the bed.

The void space represents 78% of the overall volume of the fixed bed: 39% of the volume is constituted by the interparticle space, and 39% by the pores within the pellets (23% for the macropores and mesopores and 16% for the micropores).

The adsorbate is methanol. The adsorption occurs in the micropores in which the adsorbed phase and the vapour phase are present at the same time. In the other void space (mesopores, macropores, and interparticle voids), the fluid is in the vapour state only (capillary condensation may take place in the macropores when saturation pressure is approached; this condition will not be considered in this paper).

To be rigorous in dealing with this problem, one should take into account three equations: the heat transfer equation, the mass transfer equation and the state equation of the adsorbent–adsorbate system.

Since the medium is heterogeneous and the system of partial differential equations is nonlinear, it appears useful to introduce some simplifying assumptions. This is the approach developed in the remainder of this paper.

The very high porosity of the medium (78% in volume), as well as the scale of observation to be used—several times the size of a single pellet—lead us to test a model in which we make two important assumptions:

(1) pressure is uniform (not only in the interparticle voids, but also inside the pellets themselves);

(2) the heterogeneous medium is treated as an equivalent continuous medium.

We have developed a two-dimensional numerical model (to account for the fin effect) based on the two assumptions stated above.

NOMENCLATURE

c_1 heat capacity of the metal of the heat exchanger [kJ kg^{-1} K^{-1}]
c_2 heat capacity of the solid adsorbent [kJ kg^{-1} K^{-1}]
c_3 heat capacity of the adsorbate [kJ kg^{-1} K^{-1}]
e fin thickness [m]
D coefficient of affinity in the Dubinin equation
h heat transfer coefficient between the heat exchanger and the metal [W m^{-2} K^{-1}]
H_a fin length [m]
k equivalent conductivity of the solid adsorbent [W m^{-1} K^{-1}]
k' conductivity of the metal of the heat exchanger [W m^{-1} K^{-1}]
L fin spacing [m]
m mass of adsorbate in the adsorbent [kg kg^{-1}]
n exponent in the Dubinin equation
P pressure of the adsorbate [Pa]
$P_s(T)$ saturated pressure of the adsorbate at the temperature T[Pa]
P_c condensing pressure [Pa]
P_e evaporating pressure [Pa]
Q heat source [kW m^{-3}]
Q' mass source [kg s^{-1} m^{-3}]
q_{st} latent heat of adsorption [kJ kg^{-1}]
R constant of perfect gas
t time [s]
T temperature of the adsorbent [K]
T_a ambient temperature [K]
V total volume of the reactor [m^3]
W_0 maximal capacity of the sorbent [m^3 kg^{-1}]
x x-axis perpendicular to the upper plate
y y-axis perpendicular to the fin.

Greek symbols

ρ_1 specific mass of the metal of the heat exchanger [kg m^{-3}]
ρ_2 specific mass of the solid adsorbent [kg m^{-3}]
ρ_3 specific mass of the adsorbate [kg m^{-3}].

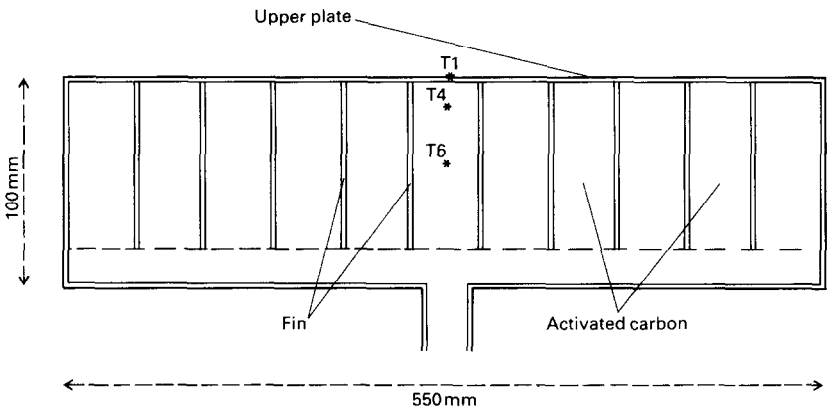

FIG. 1. Cross-section of the reactor showing the upper plate, the fins, the localization of the temperature probes * and the packing of the active carbon between the fins.

In order to validate this model, experimental measurements (temperatures and pressure) have been conducted. To compare the model and the measurements, we have been led to identify two parameters: the equivalent conductivity of the porous medium and the thermal contact resistance between the metal and solid adsorbent.

2. MATHEMATICAL MODELIZATION AND NUMERICAL RESOLUTION

2.1. *Background*

The work presented here must be situated with respect to other work being done in this field.

For a long time, this type of work has mostly dealt with isothermal diffusion [3]. Recently, however, studies in non-isothermal diffusion in a pellet have been presented [4]; Lee and Ruthven [5] have, for example, studied mass diffusion in a pellet of solid adsorbent and taken into account the thermal effects associated with adsorption; in this model, they assume that the temperature is homogeneous in the pellet but varies with time; Sun *et al.* [6], for their part, have studied coupled heat and mass transfer and have taken into account the temperature and concentration inhomogeneities within the pellet.

The non-isothermal diffusion in a bed of porous particles has been studied by Ruthven and Lee [1] in

the case where the bed mass diffusion controls the kinetics: they assume that both the thermal conductivity of the individual adsorbent particle and the effective thermal conductivity of the particle bed are large enough to maintain a uniform temperature throughout the entire adsorbent sample. This assumption should be valid when one uses very compact and thin slabs of adsorbent.

The model developed here lies upon the assumption that the bed heat conduction controls the kinetics of the sorption: we assume that the pressure is uniform in the reactor when the temperature is nonuniform. This assumption should be valid when one uses thick beds of high porosity.

The most important assumptions of our model have been experimentally validated.

(1) Pressure drops between the inlet and outlet of the bed have been measured using a differential pressure sensor: with the heat rate used in the experiment presented in that work, the pressure drop is always less than 50 Pa when the pressure is 1.2×10^4 Pa and can then be neglected.

(2) The thermodynamic equilibrium within the bed has been checked, using a flash desorption technique as used by Karagiorgas and Meunier [7]: when the reactor is submitted to a small flash desorption (corresponding to the heat rate used in solar experiments) no thermodynamic evolution of the reactor is observed after the flash desorption. On the opposite, thermodynamic evolution due to the kinetics of the adsorption is observed after very strong flash desorptions (corresponding to heat rates 100 or 1000 times higher than those used in solar energy).

2.2. *Assumptions*

(1) Mass transfer within the bed occurs only in the vapour phase. The thermodynamic equilibrium equation of the bivariant solid–gas system $m = \Gamma(\ln P, T)$ is verified at every point and at every moment: the pellets of adsorbent act like sources distributed in the reactor.

(2) The symmetry of the reactor, which makes it possible to model an elementary half-cell (cf. Fig. 2, domain ABCD).

(3) Convective heat transfer in the vapour phase is neglected.

(4) Pressure is assumed to be uniform in the reactor (grad $P = 0$).

(5) The resistance to mass diffusion through the interparticle voids and the pores is neglected.

2.3. *Equations of the system*

Let us consider a rectangular elementary cell (Fig. 2). This cell consists of a cylinder copper frame, the cross-section of which is presented in Fig. 2: a horizontal plate and vertical fins. The solid adsorbent is distributed below the horizontal plate and between the fins.

With assumption 2, the half-cell ABCD corresponds to a two-dimensional space geometry since we assume homogeneity in the z-direction.

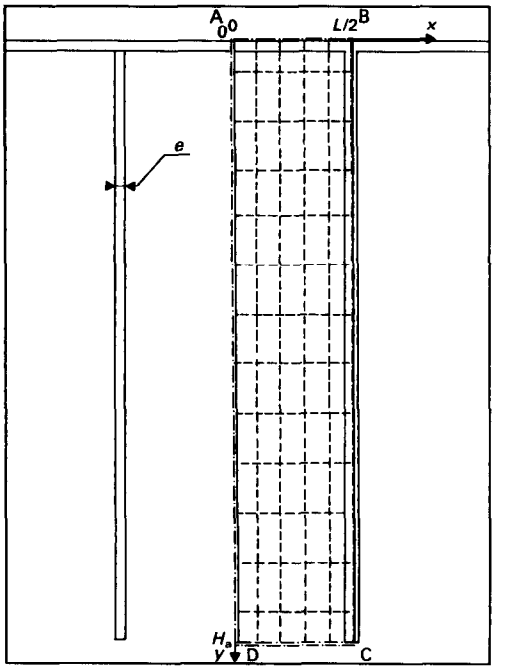

FIG. 2. Cross-section of an elementary cell in the reactor. ABCD is the half-cell used for the numerical simulation. The discontinuous lines correspond to the numerical discretization. Geometry parameters: e, fin thickness; L, fin spacing; H_a, height of the solid adsorbent bed.

The horizontal surface represented on Fig. 2 by the line AB is submitted to a heat flow. The heat diffuses into the copper parts as well as within the adsorbent layer.

2.3.1. *Energy conservation.*

For copper

$$\rho_1 c_1 \frac{\partial T}{\partial t} = k' \Delta T. \tag{1}$$

For the adsorbent layer

$$[\rho_2(c_2(T) + m(P,T)c_3(T))]\frac{\partial T}{\partial t} = k\Delta T + Q(x,y) \tag{2}$$

where $Q(x,y)$ is the two-dimensional space–time heat source term of sorption.

2.3.2 *Mass conservation.* The space–time relationship in the transfer of mass through a substance by means of diffusion and in the presence of mass sources or sinks is modelled by the following equation:

$$\rho_3 \frac{\partial m}{\partial t} = Q' \tag{3}$$

where the parabolic term has been neglected according to assumptions 4 and 5.

$Q'(x,y)$ is the two-dimensional space–time mass source term of sorption which is linked to the heat source term through the isosteric heat of sorption q_{st}

$$Q = q_{st} Q'. \tag{4}$$

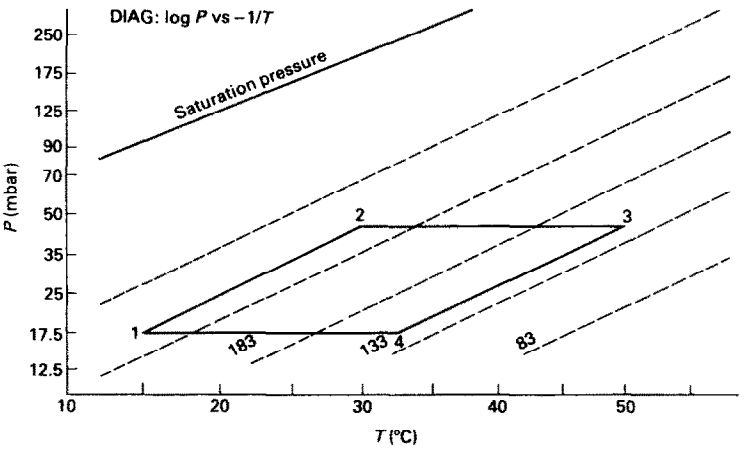

FIG. 3. Solid adsorption intermittent cycle, 1–2–3–4: 1–2–3, heating period; 1–2, isosteric period; 2–3, isobaric period.

The mass source term is obtained from the state equation of the bivariant solid–vapour equilibrium

$$m = \Gamma(\ln P, T) \tag{5}$$

where Γ is the Dubinin equation [11]

$$m = W_0 \rho_3(T) \exp\left[-D\left(T \ln \frac{P_s(T)}{P}\right)^n\right]. \tag{6}$$

Here $P_s(T)$ represents the saturating vapour pressure.

The differentiation of equation (6) gives

$$\mathrm{d}m = nDmT^n \left(\ln \frac{P_s(T)}{P}\right)^{n-1} \left[\mathrm{d}\ln P - \frac{q_{st}}{RT^2}\,\mathrm{d}T\right] \tag{7}$$

where we introduced the Clapeyron equation

$$\left(\frac{\partial \ln P}{\partial T}\right)_m = \frac{q_{st}}{RT^2}. \tag{8}$$

2.3.3. *Initial conditions.* Uniform temperature distribution

$$T(x, y, t = 0) = T_0 \tag{9}$$

$$P(x, y, t = 0) = P_0 \tag{10}$$

with conditions (9) and (10), the initial mass distribution m_0 is given by the equilibrium state equation

$$m_0 = \Gamma(\ln P_0, T_0) \tag{11}$$

and the total adsorbed mass in the reactor

$$M_0 = \rho_3(T_0) V m_0 \tag{12}$$

where ρ_3 is the specific mass of the adsorbate and V the volume of the reactor.

2.3.4. *Boundary conditions.* In the formulation of our problem, m and P are connected in explicit form through T by the state equation. In this case, the exact knowledge of the boundary conditions (on T and m or T and P) is necessary and sufficient to close the system of equations.

The system, equations (1)–(3), will be studied during the heating period of a solid adsorption cycle (Fig. 3).

It is assumed that there is a thermal resistance between the copper (upper plate or fin) and the adsorbent. If T_1 is the metal temperature and T_2, the adsorbent temperature, we can write

$$-k \left.\frac{\partial T}{\partial n}\right|_{y=e} = h(T_1 - T_2);$$

$$-k \left.\frac{\partial T}{\partial n}\right|_{x=(L-e)/2} = h(T_1 - T_2) \tag{13}$$

where $1/h$ is the contact thermal resistance between copper and adsorbent. When $x = 0$ and $L/2$, for symmetry reasons, we have

$$\left.\frac{\partial T}{\partial n}\right|_{x=0} = 0, \quad \left.\frac{\partial T}{\partial n}\right|_{x=L/2} = 0. \tag{14a}$$

When $y = H_a$, the boundary is assumed to be adiabatic

$$\left.\frac{\partial T}{\partial n}\right|_{y=H_a} = 0. \tag{14b}$$

For the upper plate

$$T(x, y = 0, t) = f(t) \tag{15}$$

where $f(t)$ is a known function of time (Dirichlet condition). For an isosteric evolution of the reactor, during which heating occurs with the reactor closed, we have

$$\frac{\mathrm{d}}{\mathrm{d}t} \int\int_{ABCDA} m\,\mathrm{d}x\,\mathrm{d}y = 0. \tag{16}$$

When the pressure reaches the condensing pressure, the reactor is connected with the condenser, which imposes its pressure to the reactor

$$P = P(t). \tag{17}$$

2.4. *Numerical resolution*

The set of coupled equations (1)–(3) is solved differently depending on boundary conditions (16) and (17).

During the isosteric period, equation (16) can be

written as

$$\frac{d}{dt}\int\int m(T(x,y),P)\,dx\,dy = 0. \quad (18)$$

Then equation (18) is applied on equation (7) with assumption 4 and we obtain

$$d\ln P = \frac{\int\int b(m,P,T)\frac{q_{st}}{RT^2}\,dT\,dz\,dy}{\int\int b(m,P,T)\,dx\,dy} \quad (19)$$

where

$$b(m,P,T) = nDmT^n\left(\ln\frac{P_s(T)}{P}\right)^{n-1}. \quad (20)$$

Then it is possible to express dm in equation (7) as a function of the temperature and recombining with equation (2), the temperature field is calculated by means of the following integro-differential non-linear equation:

$$\left[\rho_2(c_2(T)+m(P,T)c_3(T))-b(m,P,T)\frac{q_{st}}{RT^2}\right]\frac{\partial T}{\partial t} = k\Delta T+q_{st}b(m,P,T)\frac{\int\int b(m,P,T)\frac{q_{st}}{RT^2}\frac{dT}{dt}\,dx\,dy}{\int\int b(m,P,T)\,dx\,dy}. \quad (21)$$

Then, once the temperature field is known, the pressure P and the two-dimensional space concentration profile at time t are calculated respectively by means of equations (19) and (6).

During the period where the reactor is connected to the condenser, the pressure is known explicitly by means of boundary condition (17). So, it is possible to introduce expression (7) directly into equation (2). The temperature field is then determined by the following non-linear differential equation:

$$\left[\rho_2(c_2(T)+m(P,T)c_3(T))-b(m,P,T)\frac{q_{st}}{RT^2}\right]\frac{\partial T}{\partial t} = k\Delta T+q_{st}b(m,P,T)\frac{d\ln P(t)}{dt}. \quad (22)$$

Then the mass field is calculated via the state equation.

For the two periods, the set of coupled equations is solved iteratively. The solution (m,T,P) is considered as the good one if the solution for the temperature field has converged.

The numerical method uses the finite-difference technique according to a Crank–Nicholson schema. The resolution of equations (21) and (22), linearized by evaluating the coefficients at time $(n+1/2)\Delta t$, was obtained by a purely implicit schema. For the explicit method, the very great ratio between the thermal diffusivity of the copper wall and that of the bed required the use of a time step of the order of 1/1000 s, which, in view of the overall time of a complete cycle (of the order of a few hours) made the numerical simulation prohibitive.

Let us note that the matrix associated with that system of linear equations is a full matrix in 'isosteric period'. This is due to the fact that, in equation (21), the internal source term in each point depends on the state of all the points of the reactor.

The direct calculations (without identification of parameter) were carried out for 720 time steps of 10 s of the real time. The corresponding calculation time is a few seconds on an NAS 9080 computer.

3. EXPERIMENTS

3.1. *Experimental set-up*

The reactor described above is linked to a condenser (or evaporator) that makes it possible to maintain the pressure at a required value. A valve makes it possible to isolate the reactor from the condenser (or evaporator).

Our experimental cell is heated by means of an electrical element on the upper face of the reactor. The heating power is comparable to that encountered in solar-powered systems (50 W kg^{-1} of A.C. 35 activated carbon).

The transfer phenomena are studied in an elementary cell located at the centre of the reactor. The effects due to thermal losses at the edge of the reactor are negligible in this cell. Temperature probes are distributed in an elementary cell within the adsorbent bed on the fins. The pressure and temperatures are measured and recorded by a computerized data-acquisition system.

The experiment was conducted in such a way as to make the reactor reproduce the thermodynamic path of a solar collector during the heating phase of a solid-adsorption refrigeration cycle.

Figure 4 shows the history of a measured temperature and pressure (continuous line) as a function of time over the two phases of the cycle.

T_1 shows the temperature profile of the probe of the copper plate that receives the heating flow. The experimental variations in T_1 over time are used as a boundary condition of the first kind in the model.

T_4 and T_6 are two temperature probes located at the core of the reactor and on the boundary of the field under study.

Pressure is measured at the outlet of the reactor.

The absolute error on the temperature measurements is 0.3°C, while the absolute error on pressure measurement is 100 Pa.

3.2. *Experimental procedure*

In the initial state, the reactor is homogeneous in temperature under a low-pressure methanol atmosphere. Then the reactor is heated with the electrical resistance located on the upper face of the reactor.

In a first period, the reactor is closed. The heating of the upper plate induces inhomogeneities of temperature inside the reactor and causes an increase in pressure. These changes in pressure and temperature (Fig. 4) are stored by the data-acquisition system.

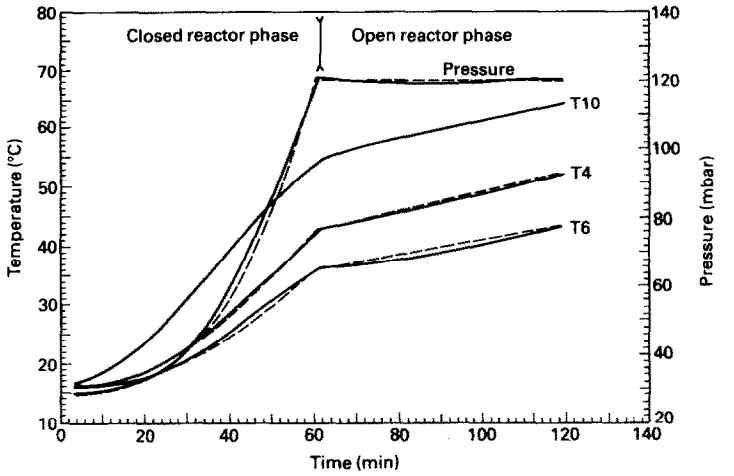

FIG. 4. History of three temperatures and the pressure during the heating period: ——, experimental results; ----, numerical results.

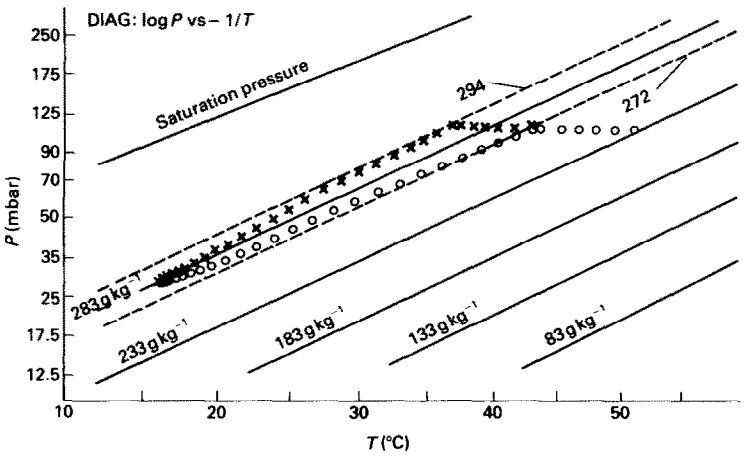

FIG. 5. Thermodynamic evolution of points 4 and 6 of the unit (Fig. 1) during the heating period.

When the pressure reaches the value of the condensing pressure, the connecting valve between the reactor and the condenser is opened.

The reactor is then an open system and desorption takes place (which causes condensation in the condenser). During this phase, the pressure is nearly constant (desorption is quasi-isobaric), while temperatures continue to increase (Fig. 4).

3.3. *Analysis of the experimental results*

The most important point is the observation of important temperature inhomogeneities and pressure homogeneity in the reactor. The consequence of this, is shown in Fig. 5, where we present the thermodynamic path of the points corresponding to the experimental readings of probes 4 and 6 in a Clapeyron diagram ($\ln p$, $-1/T$). In the closed reactor phase, probe 4 is placed in a hot zone that desorbs 11 g kg^{-1}, whereas probe 6 is placed in a colder zone that adsorbs 11 g kg^{-1}. The total mass of methanol inside the bed remains constant in the reactor, so we note a migration effect of the adsorbed methanol. This effect has an important consequence from the thermal point of view. The migration contributes to the thermal transfer by a heat pipe effect: heat is extracted from the hot zones and transferred to the colder zones.

The heat transfer takes place in two ways:

(a) by a two-dimensional conduction process through the adsorbent bed and the fins;

(b) by a heat pipe effect associated with the mass transfer.

This heat pipe effect operates in a non-stationary regime when the heat pipe is usually operated in a stationary non-equilibrium regime. The consequences of that effect are given below when one causes a temperature gradient inside a solid adsorbent fixed bed.

(1) *In a closed volume*, the bed reacts by a mass transfer that tends to counter (by virtue of the latent heat of sorption) this temperature gradient.

This heat pipe effect is similar—in the case of a divariant solid adsorbent–vapour equilibrium—to the well-known heat pipe effect resulting from the coupling between two liquid–vapour interfaces.

In these two cases, a heat transfer between a hot interface and a cold interface occurs resulting from the succession of an evaporation and a condensation. However, these two cases are distinct since in the liquid heat pipe, the temperatures of the evaporating interface and that of the condensing interface can remain constant. On the opposite, in the case of the solid adsorbent heat pipe, the two interfaces correspond to a divariant equilibrium so that at least one of the temperatures of the two interfaces (evaporator or condenser) must change for the heat pipe to work in a closed volume.

(2) *In an open volume*, the bed reacts by an inhomogeneous variation in adsorbed concentration mass that tends to counter the variation in temperature.

4. IDENTIFICATION

The numerical model established in Section 2 includes two unknown coefficients which are obtained by an identification method.

In the set of equations (2)–(15), the unknown parameters that we are going to identify with our model are the following:

(a) the equivalent conductivity of the fixed bed: k;
(b) the fin/adsorbent heat transfer coefficient: h.

The parameters (W_0, D, n) that enter into the state equation (6) and the numerical value of the isosteric heat of desorption q_{st} were determined by Boubakri *et al.* [9].

At the time of each experiment, we have recorded N values of the temperature at three points distributed in the observation space ABCD and N values P of the pressure as a function of time.

For a given pair (h, k), the numerical resolution of the system generates a particular solution $S(h,k)$ of the values of the temperatures at the points i and a solution $P(k,h)$ as a function of time.

The criterion of error can be calculated either on the temperatures or else on the pressure, or on a combination of both. We have first selected a criterion of error on the temperatures.

This criterion of error F is expressed by the mean quadratic deviation between the values of the measured temperatures T and the calculated temperatures S, i.e.

$$F(h,k) = \left(\frac{1}{3N}\sum_{j=1}^{3}\sum_{i=1}^{N}(S_{ij}-T_{ij})^2\right)^{1/2}. \qquad (23)$$

The minimization of $F(h,k)$ makes it possible to find the pair (h_0, k_0) independent of the temperature for which the model approaches the phenomenon under consideration most closely.

The minimization program uses the BOTM algorithm developed by Powell [10].

4.1. *Result of the identification*

In order to have a good evaluation of the influence of errors in measurement of the temperature on identification, we have solved the problem for the following three cases, by taking different values of T.

(1) The values of the measured temperatures, we obtain the minimum $F_{00} = 0.33$ for (h_0, k_0). Figure 6 shows the map of the iso-criteria in the plane (h,k) corresponding to that case.

(2) The values of the measured temperatures increased by positive maximum errors (+0.3°C). We have obtained the minimum of F_{01} for ($h_1 = 15.9$ W m^{-2} °C^{-1}; $k_1 = 0.197$ W m^{-1} °C^{-1}) that we project onto Fig. 6.

(3) The values of the measured temperatures decreased with negative maximum errors (−0.3°C), we have obtained the minimum F_{02} for $h_2 = 17.1$ W m^{-2} °C^{-1}; $k_2 = 0.183$ W m^{-1} °C^{-1} that we project onto Fig. 6.

The equivalent conductivity k of the active carbon–methanol pair and the coefficient of heat transfer h between fin and adsorbent are

$$k = (k_1+k_2)/2 \pm (k_1-k_2)/2 = 0.19 \pm 0.007 \text{ W m}^{-1} \text{°C}^{-1}$$

$$h = (h_1+h_2)/2 \pm (h_1-h_2)/2 = 16.5 \pm 0.6 \text{ W m}^{-2} \text{°C}^{-1}.$$

Let us note that the errors on the identified parameters are much larger than on the measured temperatures: a 0.1% error on the temperature (+0.3°C) leads to a 5% (−0.8 W m^{-2} °C^{-1}) error on the h coefficient. Nevertheless, the precision on h and k (4%) is sufficient for the use of the model.

These values may be compared to those obtained by Völkl [12] by a different technique with another system. The technique used by Völkl was a stationary state technique and the system studied was Na–Y–zeolite and water vapour.

His measurements led to values of 0.15 W m^{-1} °C^{-1} for k and values ranging from 25 to 2500 W m^{-2} °C^{-1} for h.

These results correspond to the same order of magnitude as ours and it is important to keep in mind that the results depend on the exact packing of the particles in the reactor. It is the reason why measurements performed on an apparatus with a defined geometry may lead to results different from those corresponding to a reactor with another geometry (and another packing of the pellets). We think that *in situ* identification of those coefficients is necessary for each reactor.

4.2. *Sensitivity of identification model*

The error functional can be written at point F_0 as

$$F = F_0 + \sum_{i=1}^{5}\left(\frac{\partial F}{\partial p}\right)_{i\neq p} \mathrm{d}p. \qquad (24)$$

At the minimum error we present, in Table 1, the

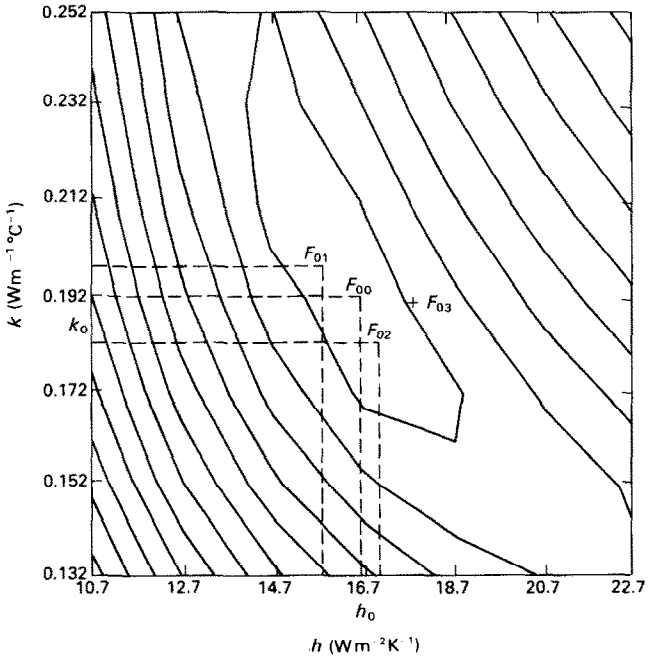

FIG. 6. Criterion of error chart vs the coefficient of heat transfer between the heat exchanger and the porous medium (x-axis) and the equivalent conductivity k of the porous medium. Interval between two lines 0.33°C.

Table 1. Values of the partial derivatives $(\partial F/\partial p)$ used in the functional error, equation (24), with the following parameters p: h, k, W_0, D, q_{st}

Parameter	Sensitivity
h	0.20
k	0.05
W_0	0.15
D	0.07
q_{st}	0.14

values of the partial derivatives of the mean quadratic deviation as a function of the transfer parameters h and k and of the physico-chemical parameters W_0, D of the solid–vapour equilibrium equation, and, finally, of the heat of desorption q_{st}.

The parameters to which the model is most sensitive are, in the order of importance:

(a) the contact thermal resistance between the fin and the adsorbent;

(b) the maximal volume W_0 offered to adsorption and the heat q_{st};

(c) the parameter D, which characterizes the affinity of the active carbon for methanol;

(d) and, finally the equivalent conductivity k of the bed.

The contact thermal resistance is the parameter to which the temperature field is most sensitive (four times more sensitive than the conduction of the bed). If one wants to decrease the inhomogeneities in the reactor, it is recommended to seek the technological means to achieve a definite decrease in the value of this contact resistance.

4.3. *Validity of the model*

Let us remember that the pair of transfer coefficients were identified by minimizing a criterion of error on the temperatures. The minimization was carried out again and independently of the previous one by calculating the criterion of error on the mean quadratic deviation between the pressure measured experimentally and the calculated pressure. The identification of h_3 and k_3 performed with the pressure gives results very close to those obtained by the previous identification $k_3 = 0.189$ W m^{-1} °C^{-1}, $h_3 =$ 18.5 W m^{-2} °C^{-1}— point F_{03} on Fig. 6.

This result is very important. First of all, it shows that the assumptions of the model are well adapted to the phenomenon. Indeed, if one of the assumptions regarding uniform pressure and the validity of the state equation at every point were not verified, we would have observed a disagreement between the two identifications.

Moreover, from an experimental point of view, the measurement of the pressure at the outlet of the reactor and the knowledge of thermal boundary conditions are sufficient to identify the two heat transfer parameters:

(a) contact resistance between the fin and the adsorbent;

(b) thermal conductivity of the microporous medium.

This makes it possible to avoid measuring temperatures inside the reactor and thus to simplify the experiments.

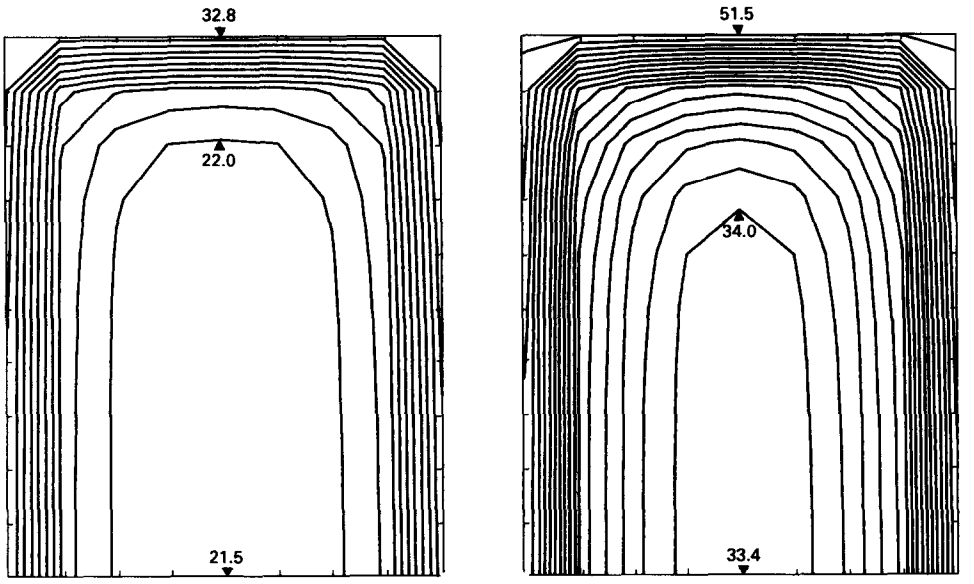

FIG. 7. Temperature mapping between two fins of the reactor: (a) during the isosteric heating; (b) at the end of the isosteric heating. Interval between two lines 1°C.

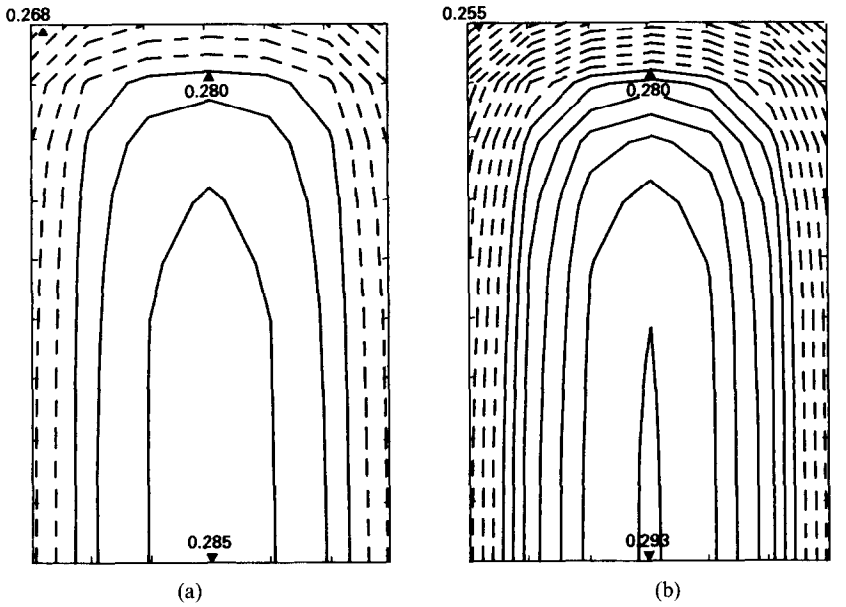

FIG. 8. Concentration mapping between two fins of the reactor: (a) during the isosteric heating; (b) at the end of the isosteric heating. Interval between two lines 0.002 g g^{-1}.

5. ANALYSIS OF THE RESULTS OF THE MODEL

5.1. *Local heat and mass balances*

In Fig. 7, we present the temperature distribution profiles between two fins of the reactor at two instants of the cycle (Fig. 3):

(a) in the middle of the isosteric heating;
(b) at the end of the isosteric heating.

The thermal gradient is higher in the neighbourhood of the metal plate of the exchanger (or the fins) and this shows the importance of the contact resistance between the fin and the adsorbent.

In Fig. 8, we present the field mass distribution profiles corresponding to the temperature field of Fig. 7. Line 0.28 represents the initial methanol content. Let us recall that the total mass of adsorbed methanol is constant in the closed reactor. During heating, a part of the adsorbed phase migrates, via the vapour phase, through a desorption–adsorption phenomenon. The zones close to the fins heat up rapidly and lose some of their methanol; this methanol migrates via the vapour phase towards the colder zones in the core of the reactor, where it is readsorbed.

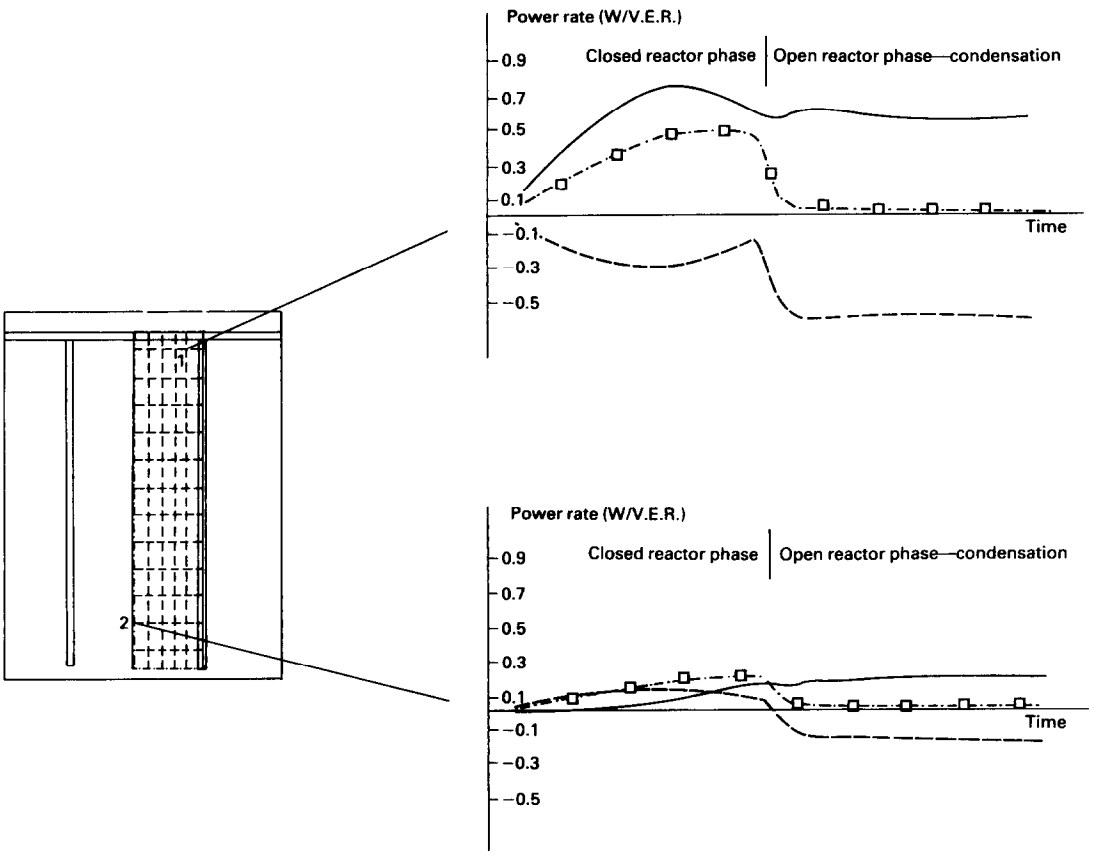

FIG. 9. Contributions to the heat transfer for two points of the reactor (1, one of the hottest points; 2, the coldest point): ——, heat rate transferred by conduction; ----, heat rate transferred by the heat pipe effect; —□—□—, sensible heat rate used to increase the temperature.

In Fig. 9, we analyze the energy contributions at the hottest point in the reactor (point 1) and at the coldest point (point 2).

We have plotted in this figure the values of the three terms of equation (2) corresponding to the total sensible heat; to the heat transmitted by conduction; and to the source term vs time.

The sum of these quantities is obviously zero.

Let us analyse in both phases (the closed-reactor and open-reactor phases) the sign of the source term and the magnitude of this term with respect to the sensible heat term.

Closed-reactor phase (increasing pressure)

Point 1. At this point, the incoming heat flux is used to raise the temperature of the adsorbent and to desorb (heat pipe effect).

Point 2. The heat of adsorption (heat pipe effect) is added to the heat transferred by conduction to heat the adsorbent.

In this phase, the desorption retards the heating of the hottest layers when adsorption accelerates the heating of the coldest layers. But there is a limit to this effect: when the coldest layers are saturated, this effect can no longer take place.

Open-reactor phase (constant pressure)

During the isobaric phase, the major part of the heat transferred by conduction is used to desorb: the temperature of the reactor increases very slowly.

5.2. *Local thermodynamic paths in a Clapeyron diagram*

It is possible to use the results of our model to establish more precisely the thermodynamic paths in a Clapeyron diagram (Fig. 10) of the various volume elements of the reactor. To do so, we shall limit our analysis to the case of the closed reactor.

The thermodynamic paths followed during a heating period—from a state of thermodynamic equilibrium—by the various volume elements of the reactor are located in a sector of the plane $(\ln P, -1/T)$ lying between the adiabatic and the isobaric lines. The various states of all the volume elements at a given instant are represented by an isobaric segment. The length of this segment—representing the magnitude of the temperature inhomogeneities—depends on various parameters, including: the thickness of the bed, the conductivity of the porous medium, the distribution of the fins in the reactor, the fluid, etc. The coldest volume element follows a path very close to an adiabatic line while the hottest volume element follows a line with an initial slope that is intermediate between the isobaric and the adiabatic lines.

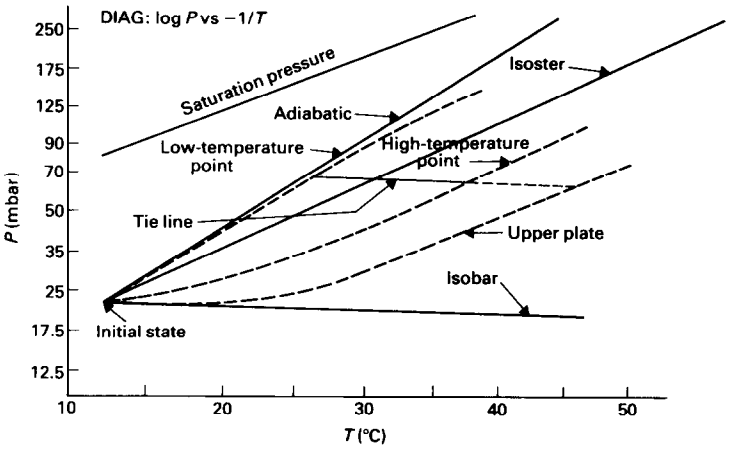

FIG. 10. Thermodynamic representation of the evolution of three points.

6. CONCLUSION

On the basis of the following assumptions:

(a) uniform pressure in the reactor;
(b) negligible mass-diffusion resistance;

we have developed a two-dimensional, numerical-simulation program that makes it possible to account for coupled heat and mass transfer phenomena via a phase transition regime in a solid-adsorbent finned reactor.

This numerical program determined the temperature and concentration fields and makes it possible to describe the significant inhomogeneity phenomena inside the reactor.

In particular, we have brought to light a heat pipe effect during the heating of the adsorbent bed in a closed reactor.

We take into account the thermodynamic and thermochemical characteristics of the reactor and two thermal transfer coefficients (equivalent conductivity of the fixed bed of adsorbent k and coefficient of transfer between fin and adsorbent h). These two coefficients have been identified $k = 0.19 \pm 0.007$ W m^{-1} °C^{-1} and $h = 16.5 \pm 0.6$ W m^{-2} °C^{-1}.

Our model is well adapted to thick beds of solid adsorbent of high porosity when uniform temperature models are not adapted to that situation but could be adapted to compact and thin slabs of adsorbent [1].

We think that in the case of a thick bed, a model based on a uniform temperature assumption as presented by Sakoda and Suzuki [8] is not at all adapted, since the temperature inhomogeneities are quite important.

The limit of our model comes from our assumption that the pellets are under equilibrium, this limit could be overtaken adding a diffusion equation for the pellets. Work is underway in that direction in our laboratory.

The exact values of the two identified parameters may depend strongly on the packing of the adsorbent in the reactor. It is the reason why it is important to keep in mind that independent measurements of these two thermophysical parameters with another reactor may lead to erroneous results. The *in situ* identification appears to be a necessary method to model with a good precision the kinetics of reactors under sorption.

It may be difficult to measure temperatures inside the reactor, but we have seen that by taking a criterion of error on pressure, identification makes it possible to determine these two coefficients by measuring only (but accurately) the history of the pressure in the reactor and that of the temperature of the external surface of the reactor which makes the identification not too heavy.

At the end of this study, we are already able to simulate numerically the operation of a reactor in a nonsteady state (temperature/pressure/mass at each point in the system) in the case of a low heat flow constraint. This model has been applied for the thermodynamic and economic optimization of solar powered solid adsorbent refrigerating units [13] as well as for the sizing of heat exchangers used in solid adsorbent heat pumps.

Acknowledgement—This work was supported by the PIR-SEM–CNRS (Programme interdisciplinaire de Recherches sur les Sciences pour l'Energie et les Matières Premières) and the AFME (Agence Française pour la Maîtrise de l'Energie).

REFERENCES

1. D. M. Ruthven and L. K. Lee, Kinetics of non-isothermal sorption: systems with bed diffusion control, *A.I.Ch.E. Jl* **27**, 654 (1981).
2. Ph. Grenier and M. Pons, Experimental and theoretical results on the use of an A.C. methanol intermittent cycle for the application to a solar-powered ice-maker, I.S.E.S. Perth Congress (1983).
3. R. M. Barrer, *Zeolites and Clay Minerals as Sorbents and Molecular Sieves*. Academic Press, New York (1978).
4. D. M. Ruthven, *Principles of Adsorption and Adsorption Processes*. Wiley Interscience, New York (1984).
5. L. K. Lee and D. M. Ruthven, Analysis of thermal effects

in adsorption rate measurements, *J. Chem. Soc. Faraday Trans. 1* **75,** 2406 (1979).
6. L. M. Sun, F. Meunier et B. Mischler, Etude des distributions de température et de concentration à l'intérieur d'un grain sphérique d'adsorbant solide soumis à un échelon de pression de vapeur adsorbable, *Int. J. Heat Mass Transfer* **29,** 1393–1406 (1986).
7. M. Karagiorgas et F. Meunier, Etude de la relaxation d'un réacteur à zéolithe pendant la désorption éclair provoquée par un échelon de pression, *Chem. Engng J.* **32,** 171–192 (1986).
8. A. Sakoda and M. Suzuki, Fundamental study on solar powered cooling system, *J. Chem. Engng Japan* **17,** 52–57 (1984).
9. A. Boubakri, Ph. Grenier and M. Pons, Utilisation du couple C.A.–méthanol pour la production de glace par énergie solaire. *Proceedings of the J.I.T.H. Conference*, C.N.R.S. Editor, Rabat (1985).
10. M. J. D. Powell, *Optimization Techniques with Fortran*, pp. 331–343. McGraw-Hill, New York (1973).
11. B. P. Bering, M. N. Dubinin and V. V. Serpinski, On thermodynamics of adsorption in micropores, *J. Colloid Interface Sci.* **38,** 185–194 (1972).
12. J. Völkl, *Proceedings of the 7th International Heat Transfer Conference*, 6–10 Sept., Munich. Hemisphere, Washington DC (1982).
13. J. J. Guilleminot and F. Meunier, Thermodynamic and economic optimization of solar powered solid adsorbent refrigerating units, *Solar Energy* (1987), in press.

TRANSFERT DE MASSE ET DE CHALEUR A L'INTERIEUR D'UN LIT FIXE, NON-ISOTHERME, D'ADSORBANT SOLIDE: EN PRESENCE DES GRADIENTS DE TEMPERATURE DANS UN CHAMP DE PRESSION UNIFORME

Résumé—Un modèle à pression uniforme décrivant les transferts de masse et de chaleur dans un réacteur à adsorption solide à lit fixe est présenté. Ce modèle néglige les résistances à la diffusion de masse mais tient compte des résistances à la diffusion de chaleur par l'intermédiaire de deux coefficients: la conductivité thermique du lit d'adsorbant solide et le coefficient de transfert entre l'adsorbant et l'ailette. Une expérience a été effectuée pour valider ce modèle, les deux coefficients de transfert ont été déterminés par une technique d'identification. Lorsque la température du réacteur fermé est modifiée à une extrémité de ce réacteur, de fortes inhomogénéités de température sont observées à l'intérieur du réacteur et le transfert de masse s'effectue par l'intermédiaire d'un effet de type caloduc: le modèle explique cet effet qui est observé expérimentalement. Ce modèle à pression uniforme est mieux adapté pour décrire l'évolution de réacteurs à adsorption solide utilisés dans les procédés thermiques que les modèles à température uniforme proposés par d'autres auteurs.

WÄRME- UND STOFFÜBERGANG IN EINEM NICHT-ISOTHERMEN FESTBETTREAKTOR: DER FALL GLEICHFÖRMIGEN DRUCKES UND UNGLEICHFÖRMIGER TEMPERATUR

Zusammenfassung—Es wird ein Modell mit gleichförmigem Druck zur Beschreibung des Wärme- und Stoffübergangs an einem festen Adsorptionsmittel in einem berippten Festbettreaktor vorgestellt. Dieses Modell vernachlässigt den Widerstand durch Stoffdiffusion. Die Wärmetransport-Widerstände werden durch zwei Koeffizienten berücksichtigt: einer für die Wärmeleitfähigkeit der adsorbierenden Stoffschüttung und einer für den Wärmeübergangskoeffizienten zwischen Schüttung und Rippen. Zur Validierung des Modells wurde ein Experiment durchgeführt. Die beiden Wärmetransportkoeffizienten wurden mit Hilfe einer Identifikationstechnik ermittelt. Wird die Temperatur an einer Seite des geschlossenen Reaktors geändert, so werden große Temperaturinhomogenitäten im Innern des Reaktors beobachtet, und der Stofftransport erfolgt auf Grund eines Wärmerohreffektes. Das Modell erklärt diesen Effekt, der experimentell beobachtet wird. Das Modell mit gleichförmigem Druck ist besser geeignet, die Abläufe in einem Festbettreaktor, wie er in thermischen Prozessen verwendet wird, zu beschreiben, als das von anderen Autoren vorgeschlagene Modell mit gleichförmiger Temperatur.

ТЕПЛО- И МАССООБМЕН В НЕИЗОТЕРМИЧЕСКОМ РЕАКТОРЕ С НЕПОДВИЖНЫМ СЛОЕМ ТВЕРДОГО АДСОРБЕНТА ПРИ ПОСТОЯННОМ ДАВЛЕНИИ И ПЕРЕМЕННОЙ ТЕМПЕРАТУРЕ

Аннотация—Предлагается модель тепло- и массообмена в неподвижном слое твердого адсорбента в оребренном реакторе при постоянном давлении. В модели не учитывается диффузионное сопротивление, а учет теплового сопротивления осуществляется с помощью двух коэффициентов: коэффициента теплопроводности слоя адсорбента и коэффициента теплообмена между слоем адсорбента и ребрами. Проведена экспериментальная проверка адекватности модели, и с помощью метода идентификации получены коэффициенты теплообмена. При изменении температуры на одной из сторон замкнутого реактора в слое возникают значительные градиенты температуры и перенос массы осуществляется как в тепловой трубе. Предлагаемая модель постоянного давления позволяет объяснить этот экспериментально наблюдаемый эффект и лучше описывает тепловые процессы в реакторах с твердым адсорбентом, чем предложенные другими аторами модели постоянной температуры.